Concentration matters: mechanistic differences of stomatal CO_2-responses at sub-ambient and above-ambient CO_2 levels in Arabidopsis

Kaspar Koolmeister[1]*, Ebe Merilo[1], Hanna Hõrak[1]*, Hannes Kollist[1]

*These authors contributed equally

[1]*Institute of Technology, University of Tartu, Nooruse 1, 50411, Tartu, Estonia*

Corresponding author contacts:

Hanna Hõrak, +37253496185, hanna.horak@ut.ee

Author ORCIDs: K.K 0000-0001-9521-9045, E.M. 0000-0003-1767-6413, H.H. 0000-0002-6392-859X, H.K. 0000-0002-6895-3583

Summary

- Stomatal pores that control plant CO_2 uptake and water loss affect global carbon and water cycles. In the era of increasing atmospheric CO_2 levels and vapor pressure deficit (VPD), it is essential to understand how these stimuli affect stomatal behaviour. It is unknown whether stomatal responses to sub-ambient and above-ambient CO_2 levels are governed by the same mechanisms and whether these responses depend on VPD.
- We studied stomatal conductance responses in Arabidopsis stomatal signalling mutants under conditions where CO_2 levels were either increased from sub-ambient to ambient (400 ppm) or from ambient to above-ambient levels under normal or elevated VPD.
- Signalling components involved in CO_2-induced stomatal closure have different roles in the sub-ambient and above-ambient CO_2 levels. The CO_2-specific regulators prominently affect sub-ambient CO_2 responses, whereas guard cell slow-type anion channel SLAC1 is more important for above-ambient CO_2-induced stomatal closure. Elevated VPD caused lower stomatal conductance and faster CO_2-responsiveness in most studied genotypes.
- Our results highlight the importance of experimental set-ups in interpreting stomatal CO_2-responsiveness, as stomatal movements under different CO_2 concentration ranges are controlled by distinct mechanisms. Sometimes

elevated CO_2 and VPD responses also interact. Hence, multi-factor treatments are needed to understand plant behaviour under future climate conditions.

Keywords 5-8: CO_2-signalling, guard cell signalling, stomatal physiology, stomatal closure, vapor pressure deficit (VPD)

Introduction

Atmospheric CO_2 concentration has nearly doubled within the past 150 years. As a result, the global average temperature has increased by 1.5°C and relative air humidity decreased across many vegetated areas (Yuan et al. 2019). Increased air temperature and decreased air humidity lead to rising values of vapor pressure deficit (VPD), the difference between actual and saturated air vapor pressures, and this increases transpiration from plants. In order to survive such conditions, plants need to adjust their water management by regulating stomatal conductance. Each stoma is composed of two guard cells and an opening formed between them; the size of the opening is controlled by increasing or decreasing guard cell turgor pressure. Guard cells adjust their turgor pressure in response to various abiotic stimuli to balance water loss and CO_2 uptake for photosynthesis. Understanding how stomata respond to changing CO_2 concentrations and increasing VPD is needed for breeding climate-ready crops.

Plant stomata close in response to elevated CO_2 concentration and open in response to decreased CO_2 concentration. Ultimately, elevated CO_2 activates S-type anion channel SLAC1, which causes rapid stomatal closure (Vahisalu et al., 2008; Negi et al., 2008). CO_2 can enter guard cells through the PIP2 plasma membrane channel or by transmembrane diffusion (Katsuhara & Hanba, 2008; Wang *et al.*, 2016). Carbonic anhydrases CA1 and CA4 accelerate the conversion of intracellular CO_2 to bicarbonate (HCO_3^-), which can act as a second messenger (Hu *et al.*, 2010). In guard cells, CO_2/HCO_3^- promotes interaction between the protein kinases MPK4/MPK12 and the Raf-like kinase HT1, leading to HT1 inhibition, which is an essential step in the regulation of stomatal responses to CO_2 (Hashimoto *et al.*, 2006; Hashimoto-Sugimoto *et al.*, 2016; Hõrak *et al.*, 2016; Jakobson *et al.*, 2016; Takahashi *et al.*, 2022; Yeh *et al.*, 2023). HT1 phosphorylates the CBC1/CBC2 Raf-like kinases that function downstream of HT1 and these Raf kinases can inhibit the S-type anion channel activation via a currently unknown mechanism (Hõrak *et al.*, 2016; Hiyama *et al.*, 2017; Hayashi *et al.*, 2020). Stomata in HT1-deficient plants do not respond to CO_2

concentration changes while carbonic anhydrase, MPK12 and SLAC1 mutants exhibit impaired stomatal CO_2 responses (Hashimoto *et al.*, 2006; Vahisalu *et al.*, 2008; Hu *et al.*, 2010; Hashimoto-Sugimoto *et al.*, 2016; Hõrak *et al.*, 2016; Jakobson *et al.*, 2016).

Elevated VPD increases transpiration; to prevent wilting, stomata close. Abscisic acid (ABA) is a drought-induced plant stress hormone and an important stomatal regulator. VPD has a direct effect on ABA concentration as increased ABA levels in angiosperms were observed 20 minutes after increasing VPD from 0.7 to 1.5 kPa (McAdam & Brodribb, 2015). Considering that ABA has a major role in angiosperm stomatal closure (Cutler *et al.*, 2010), elevated VPD might prime plant stomata for fast movements. The protein kinase OST1 and the leucine-rich receptor-like pseudokinase GHR1 are activated in the presence of ABA and trigger anion efflux through the major guard cell slow-type anion channel SLAC1 (Hua *et al.*, 2012; Brandt *et al.*, 2012; Sierla *et al.*, 2018). OST1 and GHR1 are both involved in elevated VPD- and CO_2-induced stomatal closure response (Xue *et al.*, 2011; Merilo *et al.*, 2018; Sierla *et al.*, 2018; Jalakas *et al.*, 2021b; Hsu *et al.*, 2021).

Understanding CO_2-induced plant stomatal closure responses is essential for future plant breeding. Due to changing climate conditions, it is also important to understand if and how stomatal CO_2 regulation is affected by elevated VPD levels. Under light, CO_2 concentration inside the leaf is usually below ambient levels and this causes stomatal opening. Stomata close when CO_2 concentration inside the leaf increases to ambient levels, and an additional rise in CO_2 concentration to above-ambient levels causes further stomatal closure (Brodribb *et al.*, 2009; Hõrak *et al.*, 2017). Thus, stomatal closure response exists within sub-ambient as well as in above-ambient CO_2 levels, however it is not clear whether the underlying mechanisms for these responses are the same. In some studies, CO_2-induced stomatal closure is defined as the response to an increase in CO_2 concentration from ambient to above-ambient levels (Franks & Britton-Harper, 2016; Hõrak *et al.*, 2017), while some studies use a [CO_2] change from sub-ambient to above-ambient levels (Azoulay-Shemer *et al.*, 2015; Chater *et al.*, 2015). Data from previous studies comparing CO_2 responses in ferns and angiosperms suggests that stomatal responses to CO_2 are different, when changing CO_2 levels in the sub-ambient or above-ambient ranges (Brodribb *et al.*, 2009; Hõrak *et al.*, 2017). To address the underlying mechanisms of CO_2-induced stomatal closure at different CO_2 transitions under normal and elevated VPD

conditions, we studied plants deficient either in guard cell anion channel SLAC1 and its activation (*slac1-3*, *ghr1-3*, *ost1-3*) or in the CO_2-specific stomatal signalling branch regulated by MPK12 and HT1 kinases (*mpk12-4*, *ht1-2*, *ht1-8D*) and carbonic anhydrases CA1 and CA4 (*ca1ca4*). Our results show that regulation of stomatal closure is different in sub-ambient and above-ambient CO_2 levels and it is also affected by VPD.

Materials and Methods

Plant lines and growth conditions

Arabidopsis thaliana accession Col-0 and the following mutants in the same genetic background were used for experiments: *slac1-3* (Vahisalu *et al.*, 2008), *ost1-3* (Yoshida *et al.*, 2002), *ghr1-3* (Sierla *et al.*, 2018), *ht1-2* (Hashimoto *et al.*, 2006), *ht1-8D* (Hõrak *et al.*, 2016), *mpk12-4* (Jakobson *et al.*, 2016), *ca1ca4* (Hu *et al.*, 2010). Plants were grown in 4:2:3 v/v peat:vermiculite:water mixture at 12/12 photoperiod with 150 µmol m^{-2} s^{-1} light in controlled-environment growth cabinets (AR-66LX; Percival Scientific; MCA1600, Snijders Scientific) at 70% relative humidity and day-time temperature of 23°C (VPD 0.84 kPa) and night-time temperature 18°C (VPD 0.62 kPa). Plant age at experiment time was ~25 days.

Gas-exchange measurements

Measurements of stomatal conductance were carried out with a temperature-controlled custom-built gas-exchange device (Kollist *et al.*, 2007; Hõrak *et al.*, 2017). Plants were inserted into measurement cuvettes and allowed to acclimate for 1-2 hours at normal air humidity (VPD, 0.9 kPa) or at lower air humidity (VPD, 2.3 kPa), 24°C air temperature and 400 ppm CO_2. Experiments with various CO_2 transitions were carried out and in some cases both under normal and at high VPD conditions, as shown in Fig. 1. The first CO_2 treatment was applied approximately at noon (11:30 to 12:30), stomatal conductance was always followed for 2 hours under each treatment (Fig. 1).

Data analysis

Magnitude of stomatal closure response was calculated as the absolute difference in stomatal conductance between last time point before treatment and at the end of 2 hours of treatment at a given CO_2 level (displayed as 'Change in g_s'). To provide kinetic

characteristics for stomatal responses, we classified response curves as exponential and non-exponential, the latter mostly comprising linear response curves with slower response kinetics. Response rate constants (displayed as k-values) were calculated by fitting exponential functions to response curves that behaved exponentially with GraphPad Prism 9.4.0. One-way ANOVA with Tukey *post hoc* test was used for statistical analysis as indicated in the figure legends, $p < 0.05$ were considered statistically significant. Statistical analyses were carried out with Past 4.0 (Hammer *et al.*, 2001) and Statistica 7.1 (Stat. Soft. Inc).

Results

Stomatal closure kinetics are different between 100 to 400 and 400 to 800 ppm [CO_2] transitions

We analysed stomatal responses to CO_2 in the sub-ambient and above-ambient concentration ranges in the model plant *Arabidopsis thaliana* to clarify whether these responses are controlled by the same regulators or display distinct underlying mechanisms. Four different CO_2 transition sequences were used (Fig. 1a,c,e,g); in two set-ups we applied high VPD (2.3 kPa) as an additional factor before and throughout CO_2 treatments (Fig. 1a,e). Experiments were started with ambient (400ppm) CO_2 concentration and each consecutive CO_2 treatment lasted for 2 hours. This approach allowed to investigate plant stomatal response to different CO_2 transitions – stomatal opening in response to CO_2 transition from 400 to 100 ppm (from here on referred to as 400-100) (Fig. 1a,c,g), from 800 to 400 ppm (800-400) (Fig. 1c), or from 800 to 100 ppm (800-100) (Fig. 1e), and stomatal closure in response to CO_2 transition from 100 to 400 ppm (100-400) (Fig. 1a), from 400 to 800 ppm (400-800) (Figure 1a,c,e), or from 100 to 800 ppm (100-800) (Fig. 1g).

Stomatal closure responses had clearly different response kinetics in Col-0 wild-type plants at different CO_2 transitions: the 400-800 stomatal closure was faster than 100-400 closure (Fig. 1a,b). The rapid 400-800 response was consistent throughout all experimental setups (Fig. 1a-f). The observed different kinetics of these CO_2-induced stomatal closure responses suggest that they could be regulated by different components. Stomatal opening responses to sub-ambient CO_2 levels, 400-100 (Fig. 1a-d,g,h) and 800-100 (Fig. 1e,f) had relatively low opening rates, whereas the 800-400 response, opening from above-ambient to ambient CO_2 levels, had a higher k-

value and a lower response range (Fig. 1c,d). This suggests that stomatal opening to sub-ambient CO_2 concentrations is a much stronger, albeit slower, response than stomatal opening during the above-ambient to ambient [CO_2] change, and essentially masks the latter in the 800-100 transition.

High VPD but not the order of CO_2 transitions affects stomatal CO_2 response kinetics

To study whether high VPD affects CO_2 responses we conducted the 400-100-400-800 and the 400-800-100 CO_2 transitions under conditions where plants were first acclimatized to increased VPD (2.3 kPa) for approximately three hours and then subjected to changes in CO_2 levels under the elevated VPD conditions. Under such conditions, the 400-100 increase in stomatal conductance was nearly two times faster (Fig. 1a,b); the difference was even more clear in the 800-100 response (Fig. 1e,f). Stomatal closure in sub-ambient to ambient CO_2 concentration range was also greatly enhanced with much faster kinetics of 100-400 response under high VPD conditions (Fig. 1a,b), whereas 400-800 closure kinetics was not affected by high VPD (Fig. 1a,b,e,f). These results suggest that during high VPD stress, plant stomata could be primed for faster movements in the sub-ambient to ambient CO_2 concentration range, but VPD has a minor role in above-ambient CO_2-induced stomatal closure.

In our first experiments, the 400-100 opening stimulus was applied before the 400-800 closure. To test whether the exposure to sub-ambient CO_2 levels had an effect on stomatal CO_2-responsiveness, we also applied the CO_2 transitions in reverse order (400-800-400-100, Fig. 1c). In the 400-100 transition we did not observe a difference in the stomatal opening rate between experiments, where it was the first (Fig. 1a,b,g,h) or the last transition (Fig. 1c,d). The response to the 400-800 transition appeared slightly faster in experiments, where it was the first (Fig. 1c-f) compared with when it was the last transition (Fig. 1a,b). However, there were no major effects of the order of CO_2 concentration transitions on stomatal CO_2-response kinetics.

The CO_2-specific pathway components MPK12 and carbonic anhydrases are more involved in sub-ambient to ambient than in above-ambient CO_2-induced stomatal closure

To better understand the role of the CO_2-signalling module comprising MPK12, HT1 and carbonic anhydrases CA1 and CA4 in stomatal CO_2 responses at different CO_2 levels, we analysed the *mpk12-4*, *ht1-2*, *ht1-8D*, and *ca1a4* in a similar experimental set-up as described for wild-type plants in Fig. 1a. All the CO_2-signalling mutants, except *mpk12-4*, showed either no stomatal closure (*ht1-2*, *ht1-8D*) or slow response with linear kinetics and small magnitude (*ca1ca4*) in response to the 100-400 transition (Fig. 2a,c,d). The response of *mpk12-4* to the 100-400 transition was as fast as in wild-type, but significantly smaller in magnitude (Fig. 2a,c,d). In response to the 400-800 transition, HT1 mutants were again unresponsive, whereas *mpk12-4* and *ca1ca4* plants closed their stomata with exponential kinetics; their closure response was slower than in WT, but larger in magnitude (Fig. 2a,c,d). Together, these data suggest that HT1 is crucial to initiate stomatal closure in response to CO_2 irrespective of CO_2 levels, whereas MPK12 and carbonic anhydrases are more important at sub-ambient compared with above-ambient CO_2 concentrations.

Elevated VPD led to lower stomatal conductance in all studied mutants (Fig. 2a,b), and thus smaller magnitudes of CO_2-induced changes in stomatal conductance (Fig. 2c,e). At the same time, stomatal CO_2-response kinetics tended to be faster under elevated VPD (Fig. 2d,f). However, elevated VPD did not have major effects on the patterns of CO_2-responsiveness in the CO_2-signalling mutants (Fig 2a-f). The only differences under elevated VPD were the faster exponential stomatal closure at the 100-400 transition for *ca1ca4*, and relatively faster stomatal closure in the *ca1ca4* compared with *mpk12-4* in the 400-800 transition (Fig. 2d,f). Together, these data suggest that the *ca1ca4* mutant is especially sensitive to the priming effect of elevated VPD for CO_2-induced stomatal closure kinetics.

SLAC1 and GHR1 are more important for above-ambient CO_2-induced stomatal closure

The SLAC1 anion channel is a major component in the activation of stomatal closure response. Thus, we examined CO_2 responses across different CO_2 concentration ranges in plants deficient in the SLAC1 anion channel (*slac1-3*) and in OST1 or GHR1: proteins involved in SLAC1 activation (*ost1-3*, *ghr1-3*, Fig. 3). Stomatal response rate of *slac1-3* plants was inhibited in both, 100-400 and 400-800 CO_2 transitions (Fig. 3a,d), though the latter was more affected as the response curve was linear while wild-

type plants had an exponential response curve, and linear functions are inherently slower than exponential. Yet, the magnitude of stomatal closure between wild-type Col-0 and *slac1-3* was only different in the 100-400 transition (Fig. 3c), while their 400-800 response magnitude was similar. Under elevated VPD, the 100-400 transition was not impaired in amplitude in *slac1-3*, although it was still significantly slower than in wild-type plants (Fig. 2e,f). Together, these results show that SLAC1 is important in stomatal closure in both sub-ambient and above-ambient [CO_2] ranges, but response kinetics tend to be more severely impacted in the 400-800 transition, suggesting a more prominent role for SLAC1 in ensuring fast above-ambient CO_2-induced stomatal closure.

Plants deficient in SLAC1 activation via OST1 or GHR1 also showed impaired CO_2-induced stomatal closure both in the 100-400 and 400 to 800 transitions (Fig. 3a,c,d). The *ost1-3* mutant had slow linear stomatal closure throughout the 100-400 and 400-800 transitions, whereas the *ghr1-3* response was exponential and thus faster in both 100-400 and 400-800 transitions (Fig. 3a,d). However, the 400-800 transition, although fast, was lower in magnitude in *ghr1-3* compared with *ost1-3* (Fig. 3a,c). Thus, both SLAC1-activating proteins are involved in CO_2 responses in all tested concentration ranges, but GHR1, like SLAC1, appears to have a more prominent role in above-ambient CO_2-induced stomatal closure.

As in other mutants (Fig. 2), elevated VPD lowered stomatal conductance and stomatal response magnitude, but increased response rate (Fig. 3). A remarkable exception was *ghr1-3*: stomatal response to 400-800 was completely missing under elevated VPD in *ghr1-3* (Fig. 3b,e).

Low CO_2-induced stomatal opening kinetics is impaired in the CO_2-signalling module and affected by VPD in plants defective in SLAC1-activation

Both the amplitude and the rate of stomatal opening in the 400-100 transition were impaired in all studied CO_2-signalling mutants irrespective of VPD (Fig. 2c,d,e,f). Thus, the CO_2-specific signalling pathway is essential for stomatal opening in the sub-ambient CO_2 levels. However, neither the amplitude nor the rate of low CO_2-induced stomatal opening in the 400-100 transition was affected in the *slac1-3* and *ghr1-3* mutants; whereas opening rate was linear and hence lower in the *ost1-3* mutants under normal VPD (Fig. 3c,d). Therefore, regulation of SLAC1 is less important for sub-

ambient CO_2-induced stomatal opening than the guard cell CO_2-specific signalling pathway. However, under elevated VPD, the 400-100 transition response was slower compared with WT in *slac1-3*, *ghr1-3* and *ost1-3* (Fig. 3f), indicating an interaction between CO_2 and VPD signalling in stomatal opening responses.

Shifting CO_2 levels from 100 to 800 ppm masks the differences between stomatal behaviour in 100-400 and 400-800 ppm [CO_2] transitions

In experiments where CO_2 concentrations were changed directly from 100 ppm to 800 ppm, the differences in closure responses that were detected for 100-400 and 400-800 transitions shown in Fig. 2 and 3, were masked (Fig. 4). In the 100-400 reaction the *ca1ca4* mutants had slow linear stomatal response, while 400-800 reaction was faster and exponential, albeit still slower than in wild-type plants (Fig. 2a,d). When we changed CO_2 concentration from sub-ambient straight to above-ambient we observed an exponential response for *ca1ca4* plants (Fig. 4a,d) – previously clearly different responses were merged into one. With *mpk12-4* plants we again observed a clear difference between 100-400 and 400-800 responses: while 100-400 response rate was similar to wild-type plants, the response was significantly smaller in magnitude, yet the 400-800 response was significantly larger in magnitude but slower than in wild-type plants (Fig. 2a,c,d). Response to the 100-800 reaction was a mix-up of 100-400 and 400-800 results, having wild-type-like magnitude while being significantly slower (Fig. 4a,c,d). In case of *ghr1-3*, slower than wild-type stomatal response was observed in both 100-400 and 400-800 reactions (Fig. 3d), whereas in the 100-800 reaction *ghr1-3* had response rate similar to wild-type plants (Fig. 4f). These results demonstrate that key differences in stomatal responses can remain undiscovered depending on CO_2 concentrations that are used for experiments.

Similar to CO_2-induced stomatal closure experiments, [CO_2] ranges were important also in stomatal opening assays (Fig. 2-3 vs Fig. 5). For example, response to the 400-100 transition in *mpk12-4* was slower and smaller in magnitude compared with wild-type plants (Fig 2c,d), but in the 800-100 experiments, *mpk12-4* had normal response amplitude and wild-type-like rate (Fig. 5c,d). The *slac1-3* plants had similar to wild-type 400-100 stomatal opening rate and magnitude (Fig. 3c,d), but were slower in the 800-100 response (Fig. 5f). We also observed a significantly slower opening response to the 800-400 transition in *slac1-3* (Supplementary Fig. 1f), which indicates that the

reduced rate of the 800-100 response in this mutant is caused by slower opening in the 800-400 range. Thus, although wild-type plants have no discernible differences between the 400-100 and the 800-100 stomatal opening responses, the molecular mechanisms involved are not the same for these CO_2 transitions.

Discussion

Here we show that stomatal closure in response to an increase in CO_2 concentration, which occurs both at sub-ambient and above-ambient CO_2 concentration ranges, comprises two different underlying processes. Stomatal closure in response to the 400-800 CO_2 concentration range is faster (Fig. 1b), while the 100-400 response has greater amplitude (Fig. 1a, 2c). The relative contribution of the components involved in stomatal CO_2-signalling is also different in these responses (Figures 2-3). Increasing CO_2 abruptly from 100 to 800 masked the presence of two processes with different kinetics (Figures 2, 3 and 4), indicating the necessity to analyse stomatal closure responses to elevated CO_2 levels separately in the ambient to above-ambient and sub-ambient to ambient CO_2 concentration ranges.

The HT1 kinase is required for plant stomatal CO_2 signalling; plants with impaired HT1 function are insensitive to all CO_2 concentration changes (Hashimoto *et al.*, 2006; Hashimoto-Sugimoto *et al.*, 2016; Hõrak *et al.*, 2016). HT1 together with MPK12 or MPK4 forms a primary CO_2 sensing complex, where CO_2/bicarbonate triggers interaction of MPKs with HT1 and this leads to inhibition of the HT1 kinase activity (Takahashi *et al.*, 2022). In our experiments, *mpk12-4* plants had disrupted stomatal response amplitude to the 100-400 CO_2 transition, while the 400-800 amplitude was largely unaffected (Fig. 2a,c). In Tõldsepp *et al,* (2018) *mpk12 mpk4GC* double-mutants, where MPK4 expression is suppressed only in guard cells, had no 400-800 CO_2 response, yet *mpk4GC* single-mutants responded to the 400-800 CO_2 transition similar to wild-type plants. Takahashi *et al.* (2022) showed MPK12 mutants to have the 400-800 response similar to current study, although neither of these studies tested the 100-400 response. Thus, it seems that the MPK12/MPK4-HT1 complex loses functionality if HT1 is impaired (Fig. 2), same happens if both MPK12 and MPK4 are missing from guard cells (Tõldsepp *et al.*, 2018), but losing only MPK12 preferentially affects the 100-400 CO_2 transition (Fig. 2). Therefore, while in the 400-800 transition the lack of MPK12 is likely compensated by MPK4, MPK4 cannot effectively replace

the function of MPK12 at sub-ambient CO_2 levels. This could mean that while MPK12 and MPK4 both can form CO_2/bicarbonate sensing complex with HT1, their affinity for CO_2/bicarbonate may be different.

CA1 and CA4 also affected stomatal responsiveness more in the 100-400 CO_2 range, with slow and shallow stomatal response in the *ca1ca4* mutant (Fig. 2). The strong stomatal closure in above-ambient 400-800 CO_2 transition in this mutant (Fig. 2) might be related to increased autonomous CO_2 conversion to HCO_3^- in the elevated CO_2 environment or by involvement of other carbonic anhydrases, as recently demonstrated (Sun *et al.*, 2022).

SLAC1 is important for stomatal closure responses to both elevated CO_2 transitions, but the response kinetics of 400-800 transition was more affected than in the 100-400 transition (Fig. 3a,d). In *slac1-3* plants there was very little stomatal closure or opening in the 400-800-400 CO_2 transitions, yet stomatal opening in response to the 400-100 transition was strong and similar to wild-type plants (Supplementary Fig. 1b), further supporting the major role of SLAC1 in stomatal responses under ambient to above-ambient CO_2 concentration changes. In the 100-400 CO_2 transition, stomatal responsiveness may be partly compensated by other ion channels that are functional in *slac1-3*. In addition to the S-type anion channels like SLAC1, stomatal closure is also affected by R-type anion channels, such as QUAC1 (Meyer *et al.*, 2010; Imes *et al.*, 2013). Jalakas *et al.* (2021a) demonstrated that the *quac1-1 slac1-3* double mutant and *quac1-1 slac1-3 slah1-3* triple-mutant had no response to the 400-800 CO_2 transition, while individually *slac1-3* had a weak response and *quac1-1* stomatal response was similar to wild-type plants. SLAH3 is another S-type anion channel contributing to stomatal closure (Zhang *et al.*, 2016) and could potentially compensate for the lack of SLAC1 in the 100-400 CO_2 response, although it does not affect the 400-800 stomatal CO_2 response (Jalakas *et al.*, 2021a). Future studies should address the 100-400 CO_2 response in mutants deficient in major S- and R-type anion channels to better understand their potential role in the 100-400 CO_2 response.

Stomatal opening triggered by decreased CO_2 levels, from 400 to 100 and from 800 to 100, had larger magnitude than the 800-400 response (Fig. 1a,c,e,g). Responses to 100 ppm final CO_2 concentration had a consistently large amplitude and slow response rate in different experimental set-ups and were not affected by the order of CO_2

treatments. Thus, stomatal opening in response to sub-ambient CO_2 concentrations is a very prominent response. This is in line with Merilo *et al*., (2014), where two stimuli with an opposing effect on stomata were simultaneously applied, such as darkness and low CO_2, or low CO_2 and elevated VPD. In such combinations, Arabidopsis stomata always opened in response to sub-ambient CO_2 levels, further indicating that reduction of CO_2 is a strong and prevailing signal. The sub-ambient CO_2-induced stomatal opening, similar to light-induced opening, likely involves H^+ATPase activation (Inoue & Kinoshita, 2017), changes in sugar and starch metabolism (Flütsch & Santelia, 2021), and suppression of stomatal closure via e.g. inhibiting anion channel activation (Marten *et al.*, 2007). The combined activation of all these processes may explain the slow stomatal opening rate in response to sub-ambient CO_2 levels.

Elevated VPD strongly lowered steady-state stomatal conductance and enhanced stomatal response rate in 400-100, 100-400 and 800-100 CO_2 concentration transitions (Fig. 1a,b,e,f). Thus, elevated VPD can act as a priming factor for plant stomatal CO_2 responses. Faster stomatal closure may be caused by increased ABA levels under elevated VPD conditions (McAdam & Brodribb, 2015). Alternatively, both faster stomatal opening and closure responses under elevated VPD may be due to smaller steady-state stomatal conductance caused by smaller apertures that can adjust faster in response to environmental changes. Steady-states of stomatal conductance of all plant lines were decreased by elevated VPD (Fig. 2b, 3b), confirming that VPD is an important factor for steady-state stomatal conductance (López *et al.*, 2021). Mutants with disrupted stomatal ABA response, *ghr1-3*, *ost1-3* and *slac1-3*, also had lower steady-state stomatal conductances under elevated VPD (Fig. 3). Their high VPD-induced decrease in steady-state stomatal conductance could be caused by ABA-independent active processes (e.g. ABA-independent OST1 activation, whose contribution to stomatal closure under high VPD increases in time according to Jalakas et al., (2021b)), or hydropassive stomatal closure. CO_2-induced stomatal responses under elevated VPD were mostly faster and had a smaller amplitude (Fig. 2b,e,f and 3b,e,f). However, response to the 400-800 CO_2 transition disappeared completely in the *ghr1-3* plants under elevated VPD conditions (Fig. 3b). GHR1 contributes to stomatal closure in response to both elevated VPD (Hsu *et al.*, 2021) and CO_2 (Hõrak *et al.*, 2016; Sierla *et al.*, 2018). This suggests that CO_2 and VPD responses may

interact in *ghr1-3*: if stomatal closure already occurred in the *ghr1-3* plants subjected to elevated VPD, no further response to CO_2 elevation was triggered.

Elevated temperatures caused by climate change increase atmospheric dryness manifested as higher VPD levels, which increases transpiration, and triggers stomatal closure to avoid wilting. Together, changes in atmospheric VPD and CO_2 levels are perhaps the greatest agricultural challenges of the future, yet how both these stimuli together affect plant stomatal behaviour is poorly understood. Here we show that while elevated VPD negatively affects steady-state stomatal conductances, it has little effect on stomatal CO_2-responsiveness. Nevertheless, in some genetic backgrounds, we found an interaction between CO_2 and VPD treatments, indicating that the simultaneous effects of these factors on stomatal behaviour merit further study. We also show that stomatal response to elevated CO_2 has different kinetics and employs different molecular mechanisms under sub-ambient and above-ambient CO_2 concentration ranges. Thus, to better understand stomatal responses to CO_2 it is necessary to carefully consider CO_2 levels and experimental set-ups.

Acknowledgements

This work was supported by the Estonian Research Council grant PSG404 to H.H., Basic funding from the Institute of Technology, PRG719, and PRG1620 to E.M. and PRG433 to H.K.; and European Regional Development Fund via Center of Excellence in Molecular Cell Engineering.

Author Contributions

H.H. designed the study, H.H., K.K. and E.M. performed experiments, H.H., K.K., E.M. and H.K. analysed data, H.H., K.K. and H.K. wrote the manuscript, all authors commented, edited and approved the final manuscript.

Data availability

Raw data is available from corresponding author upon request.

References

Azoulay-Shemer T, Palomares A, Bagheri A, Israelsson-Nordstrom M, Engineer CB, Bargmann BOR, Stephan AB, Schroeder JI. **2015**. Guard cell photosynthesis

is critical for stomatal turgor production, yet does not directly mediate CO_2- and ABA-induced stomatal closing. *The Plant Journal* **83**: 567–581.

Brandt B, Brodsky DE, Xue S, Negi J, Iba K, Kangasjärvi J, Ghassemian M, Stephan AB, Hu H, Schroeder JI. **2012**. Reconstitution of abscisic acid activation of SLAC1 anion channel by CPK6 and OST1 kinases and branched ABI1 PP2C phosphatase action. *Proceedings of the National Academy of Sciences* **109**: 10593–10598.

Brodribb TJ, McAdam SAM, Jordan GJ, Feild TS. **2009**. Evolution of stomatal responsiveness to CO_2 and optimization of water-use efficiency among land plants. *New Phytologist* **183**: 839–847.

Chater C, Peng K, Movahedi M, Dunn JA, Walker HJ, Liang Y-K, McLachlan DH, Casson S, Isner JC, Wilson I, *et al.* 2015. Elevated CO_2-Induced Responses in Stomata Require ABA and ABA Signaling. *Current Biology* **25**: 2709–2716.

Cutler SR, Rodriguez PL, Finkelstein RR, Abrams SR. **2010**. Abscisic Acid: Emergence of a Core Signaling Network. *Annual Review of Plant Biology* **61**: 651–679.

Flütsch S, Santelia D. **2021**. Mesophyll-derived sugars are positive regulators of light-driven stomatal opening. *New Phytologist* **230**: 1754–1760.

Franks PJ, Britton-Harper ZJ. **2016**. No evidence of general CO_2 insensitivity in ferns: one stomatal control mechanism for all land plants? *New Phytologist* **211**: 819–827.

Hammer O, Harper DAT, Ryan PD. **2001**. PAST: Paleontological Statistics Software Package for Education and Data Analysis. *Palaeontologia Electronica* **4**: 10.

Hashimoto M, Negi J, Young J, Israelsson M, Schroeder JI, Iba K. **2006**. Arabidopsis HT1 kinase controls stomatal movements in response to CO_2. *Nature Cell Biology* **8**: 391–397.

Hashimoto-Sugimoto M, Negi J, Monda K, Higaki T, Isogai Y, Nakano T, Hasezawa S, Iba K. **2016**. Dominant and recessive mutations in the Raf-like kinase *HT1* gene completely disrupt stomatal responses to CO_2 in Arabidopsis. *Journal of Experimental Botany* **67**: 3251–3261.

Hayashi M, Sugimoto H, Takahashi H, Seki M, Shinozaki K, Sawasaki T, Kinoshita T, Inoue S. **2020**. Raf-like kinases CBC1 and CBC2 negatively regulate stomatal opening by negatively regulating plasma membrane H + -ATPase phosphorylation in Arabidopsis. *Photochemical & Photobiological Sciences* **19**: 88–98.

Hiyama A, Takemiya A, Munemasa S, Okuma E, Sugiyama N, Tada Y, Murata Y, Shimazaki K. **2017**. Blue light and CO 2 signals converge to regulate light-induced stomatal opening. *Nature Communications* **8**: 1–13.

Hõrak H, Kollist H, Merilo E. **2017**. Fern Stomatal Responses to ABA and CO_2 Depend on Species and Growth Conditions. *Plant Physiology* **174**: 672–679.

Hõrak H, Sierla M, Tõldsepp K, Wang C, Wang Y-S, Nuhkat M, Valk E, Pechter P, Merilo E, Salojärvi J, *et al.* 2016. A Dominant Mutation in the HT1 Kinase Uncovers Roles of MAP Kinases and GHR1 in CO_2-Induced Stomatal Closure. *The Plant Cell* **28**: 2493–2509.

Hsu P-K, Takahashi Y, Merilo E, Costa A, Zhang L, Kernig K, Lee KH, Schroeder JI. **2021**. Raf-like kinases and receptor-like (pseudo)kinase GHR1 are required for stomatal vapor pressure difference response. *Proceedings of the National Academy of Sciences* **118**: e2107280118.

Hu H, Boisson-Dernier A, Israelsson-Nordström M, Böhmer M, Xue S, Ries A, Godoski J, Kuhn JM, Schroeder JI. **2010**. Carbonic anhydrases are upstream regulators of CO_2-controlled stomatal movements in guard cells. *Nature Cell Biology* **12**: 87–93.

Hua D, Wang C, He J, Liao H, Duan Y, Zhu Z, Guo Y, Chen Z, Gong Z. **2012**. A Plasma Membrane Receptor Kinase, GHR1, Mediates Abscisic Acid- and Hydrogen Peroxide-Regulated Stomatal Movement in *Arabidopsis*. *The Plant Cell Online* **24**: 2546–2561.

Imes D, Mumm P, Böhm J, Al-Rasheid KAS, Marten I, Geiger D, Hedrich R. **2013**. Open stomata 1 (OST1) kinase controls R–type anion channel QUAC1 in Arabidopsis guard cells. *The Plant Journal* **74**: 372–382.

Inoue S, Kinoshita T. **2017**. Blue Light Regulation of Stomatal Opening and the Plasma Membrane H^+-ATPase. *Plant Physiology* **174**: 531–538.

Jakobson L, Vaahtera L, Tõldsepp K, Nuhkat M, Wang C, Wang Y-S, Hõrak H, Valk E, Pechter P, Sindarovska Y, *et al.* 2016. Natural Variation in *Arabidopsis* Cvi-0 Accession Reveals an Important Role of MPK12 in Guard Cell CO_2 Signaling. *PLOS Biology* **14**: e2000322.

Jalakas P, Nuhkat M, Vahisalu T, Merilo E, Brosché M, Kollist H. **2021a**. Combined action of guard cell plasma membrane rapid- and slow-type anion channels in stomatal regulation. *Plant Physiology* **187**: 2126–2133.

Jalakas P, Takahashi Y, Waadt R, Schroeder JI, Merilo E. **2021b**. Molecular mechanisms of stomatal closure in response to rising vapour pressure deficit. *New Phytologist* **232**: 468–475.

Katsuhara M, Hanba YT. **2008**. Barley plasma membrane intrinsic proteins (PIP Aquaporins) as water and CO2 transporters. *Pflügers Archiv - European Journal of Physiology* **456**: 687–691.

Kollist T, Moldau H, Rasulov B, Oja V, Rämma H, Hüve K, Jaspers P, Kangasjärvi J, Kollist H. **2007**. A novel device detects a rapid ozone-induced transient stomatal closure in intact Arabidopsis and its absence in abi2 mutant. *Physiologia Plantarum* **129**: 796–803.

López J, Way DA, Sadok W. **2021**. Systemic effects of rising atmospheric vapor pressure deficit on plant physiology and productivity. *Global Change Biology* **27**: 1704–1720.

Marten H, Hedrich R, Roelfsema MRG. **2007**. Blue light inhibits guard cell plasma membrane anion channels in a phototropin-dependent manner. *The Plant Journal* **50**: 29–39.

McAdam SAM, Brodribb TJ. **2015**. The Evolution of Mechanisms Driving the Stomatal Response to Vapor Pressure Deficit. *Plant Physiology* **167**: 833–843.

Merilo E, Yarmolinsky D, Jalakas P, Parik H, Tulva I, Rasulov B, Kilk K, Kollist H. **2018**. Stomatal VPD Response: There Is More to the Story Than ABA. *Plant Physiology* **176**: 851–864.

Meyer S, Mumm P, Imes D, Endler A, Weder B, Al-Rasheid KAS, Geiger D, Marten I, Martinoia E, Hedrich R. **2010**. AtALMT12 represents an R-type anion channel required for stomatal movement in Arabidopsis guard cells. *The Plant Journal* **63**: 1054–1062.

Sierla M, Hõrak H, Overmyer K, Waszczak C, Yarmolinsky D, Maierhofer T, Vainonen JP, Salojärvi J, Denessiouk K, Laanemets K, *et al.* 2018. The Receptor-like Pseudokinase GHR1 Is Required for Stomatal Closure. *The Plant Cell* **30**: 2813–2837.

Sun P, Isner J-C, Coupel-Ledru A, Zhang Q, Pridgeon AJ, He Y, Menguer PK, Miller AJ, Sanders D, Mcgrath SP, *et al.* 2022. Countering elevated CO2 induced Fe and Zn reduction in Arabidopsis seeds. *New Phytologist* **235**: 1796–1806.

Takahashi Y, Bosmans KC, Hsu P-K, Paul K, Seitz C, Yeh C-Y, Wang Y-S, Yarmolinsky D, Sierla M, Vahisalu T, *et al.* 2022. Stomatal CO2/bicarbonate sensor consists of two interacting protein kinases, Raf-like HT1 and non-kinase-activity requiring MPK12/MPK4. *Science Advances* **8**: eabq6161.

Tõldsepp K, Zhang J, Takahashi Y, Sindarovska Y, Hõrak H, Ceciliato PHO, Koolmeister K, Wang Y-S, Vaahtera L, Jakobson L, *et al.* 2018. Mitogen-activated protein kinases MPK4 and MPK12 are key components mediating CO2-induced stomatal movements. *The Plant Journal* **96**: 1018–1035.

Vahisalu T, Kollist H, Wang Y-F, Nishimura N, Chan W-Y, Valerio G, Lamminmäki A, Brosché M, Moldau H, Desikan R, *et al.* 2008. SLAC1 is required for plant guard cell S-type anion channel function in stomatal signalling. *Nature* **452**: 487–491.

Wang C, Hu H, Qin X, Zeise B, Xu D, Rappel W-J, Boron WF, Schroeder JI. **2016**. Reconstitution of CO_2 Regulation of SLAC1 Anion Channel and Function of CO_2-Permeable PIP2;1 Aquaporin as CARBONIC ANHYDRASE4 Interactor. *The Plant Cell* **28**: 568–582.

Xue S, Hu H, Ries A, Merilo E, Kollist H, Schroeder JI. **2011**. Central functions of bicarbonate in S-type anion channel activation and OST1 protein kinase in CO_2 signal transduction in guard cell. *The EMBO Journal* **30**: 1645–1658.

Yeh C-Y, Wang Y-S, Takahashi Y, Kuusk K, Paul K, Arjus T, Yadlos O, Schroeder JI, Ilves I, Garcia-Sosa AT, *et al.* 2023. MPK12 in stomatal CO2 signaling: function beyond its kinase activity. : 2023.01.31.526436.

Yoshida R, Hobo T, Ichimura K, Mizoguchi T, Takahashi F, Aronso J, Ecker JR, Shinozaki K. **2002**. ABA-Activated SnRK2 Protein Kinase is Required for Dehydration Stress Signaling in *Arabidopsis*. *Plant and Cell Physiology* **43**: 1473–1483.

Zhang A, Ren H-M, Tan Y-Q, Qi G-N, Yao F-Y, Wu G-L, Yang L-W, Hussain J, Sun S-J, Wang Y-F. **2016**. S-Type Anion Channels SLAC1 and SLAH3 Function as Essential Negative Regulators of Inward K+ Channels and Stomatal Opening in Arabidopsis. *The Plant Cell* **28**: 949–965.

Figure Legends

Figure 1. Kinetics of CO_2-induced stomatal responses in wild-type Arabidopsis with regular and elevated VPD.

Col-0 wild-type Arabidopsis stomatal response to sequential changes in CO_2 concentration under regular **(a,c,e,g)** and elevated **(a,e)** VPD conditions. Mean stomatal conductance ± SEM is shown. **(b,d,f,h)** Boxplot of fitted k-values (rate constants) of stomatal response to CO_2 concentration changes. Boxes represent 25-75 % quartiles and median as the horizontal lines, whiskers indicate the smallest and largest values, points show individual plant values. **(b,f)** Statistically significantly different groups are indicated with different letters (Two-way ANOVA with Tukey *post-hoc* test). **(d,h)** Statistically significantly different groups are indicated with different letters (One-way ANOVA with Tukey *post-hoc* test). Sample size was 5 in **(a,b,c,d,e,f)** and 14 in **(g,h)**. Start of first treatment was between 11:30 to 12:30.

Figure 2. CO_2 pathway mutants retain response patterns under regular and elevated VPD conditions

(a) and **(b)** Stomatal response to CO_2 concentration changes from 400 to 100 ppm, 100 to 400 ppm and 400 to 800 ppm under regular **(a)** and elevated **(b)** VPD conditions, mean stomatal conductance ± SEM is shown. **(c,e)** Boxplot of stomatal conductance (g_s) change (mmol m^{-2} s^{-1}) in response to CO_2 concentration changes from 400 to 100 ppm, 100 to 400 ppm and 400 to 800 ppm, respectively. **(d,f)** Boxplot of fitted k-values (rate constants) of stomatal response to CO_2 concentration changes from 400 to 100 ppm, 100 to 400 ppm and 400 to 800 ppm, respectively, linear responses are marked as NA (not applicable). **(c-f)** Boxes represent 25-75 % quartiles and median as the horizontal lines, whiskers indicate the smallest and largest values, points show

individual plant values. Statistically significantly different groups are marked with different letters (One-way ANOVA with Tukey *post hoc* test). **(a-f)** Sample size was 5 for all plant lines. VPD during experiments was 0.9 kPa in **(a,c,d)** and 2.3 kPa in **(b,e,f)**. Start of first treatment was between 11:30 to 12:30. Col-0 data is same as used in figure 1, experiments with Col-0 and mutant lines were done together.

Figure 3. CO_2 response patterns in anion channel activation mutants are affected by VPD conditions

(a) and **(b)** Stomatal response to CO_2 concentration changes from 400 to 100 ppm, 100 to 400 ppm and 400 to 800 ppm in regular **(a)** and elevated **(b)** VPD conditions, mean stomatal conductance ± SEM is shown. **(c,e)** Boxplot of stomatal conductance (g_s) change (mmol m^{-2} s^{-1}) in response to CO_2 concentration changes from 400 to 100 ppm, 100 to 400 ppm and 400 to 800 ppm, respectively. **(d,f)** Boxplot of fitted k-values (rate constants) of stomatal response to CO_2 concentration changes from 400 to 100 ppm, 100 to 400 ppm and 400 to 800 ppm, respectively, linear responses are marked as NA (not applicable). **(c-f)** Boxes represent 25-75 % quartiles and median as the horizontal lines, whiskers indicate the smallest and largest values, points show individual plant values. Statistically significantly different groups are marked with different letters (One-way ANOVA with Tukey *post hoc* test). **(a-f)** Sample size was 5 for all plant lines. VPD during experiments was 0.9 kPa in **(a,c,d)** and 2.3 kPa in **(b,e,f)**. Start of first treatment was between 11:30 to 12:30. Col-0 data is same as used in figure 1, experiments with Col-0 and mutant lines were done together.

Figure 4. CO_2 transition from 100 to 800 ppm masks different responses present in 100 to 400 and 400 to 800 ppm CO_2 transitions

(a) and **(b)** Stomatal response to CO_2 concentration changes from 400 to 100 ppm and 100 to 800 ppm, mean stomatal conductance ± SEM is shown. **(c,e)** Boxplot of stomatal conductance (g_s) change (mmol m^{-2} s^{-1}) in response to CO_2 concentration changes from 400 to 100 ppm and 100 to 800 ppm, respectively. **(d,f)** Boxplot of fitted k-values (rate constants) of stomatal response to CO_2 concentration changes from 400 to 100 ppm and 100 to 800 ppm, respectively, linear responses are marked as NA (not applicable). **(c-f)** Boxes represent 25-75 % quartiles and median as the horizontal lines, whiskers indicate the smallest and largest values, points show individual plant values. Statistically significantly different groups are marked with different letters (One-way

ANOVA with Tukey *post hoc* test). **(a-f)** Sample size was 14 for Col-0; 6 for *ht1-2*; 7 for *ht1-8D*; 8 for *ghr1-3*, *mpk12-4* and *ost1-3*; 9 for *slac1-3* and *ca1ca4*. VPD during experiments was 0.9 kPa in **(a-f)**. Start of first treatment was between 11:30 to 12:30. Col-0 data is same as used in figure 1, experiments with Col-0 and mutant lines were done together.

Figure 5. Stomatal opening in 800 to 100 ppm CO_2 transition masks different responses present in sub-ambient and above ambient CO_2 concentrations

(a) and **(b)** Stomatal response to CO_2 concentration changes from 400 to 800 ppm and 800 to 100 ppm, mean stomatal conductance ± SEM is shown. **(c,e)** Boxplot of stomatal conductance (g_s) change (mmol m^{-2} s^{-1}) in response to CO_2 concentration changes from 400 to 800 ppm and 800 to 100 ppm, respectively. **(d,f)** Boxplot of fitted k-values (rate constants) of stomatal response to CO_2 concentration changes from 400 to 800 ppm and 800 to 100 ppm, respectively, linear responses are marked as NA (not applicable). **(c-f)** Boxes represent 25-75 % quartiles and median as the horizontal lines, whiskers indicate the smallest and largest values, points show individual plant values. Statistically significantly different groups are marked with different letters (One-way ANOVA with Tukey *post hoc* test). **(a-f)** Sample size was 5 for all plant lines. VPD during experiments was 0.9 kPa in **(a-f)**. Start of first treatment was between 11:30 to 12:30. Col-0 data is same as used in figure 1, experiments with Col-0 and mutant lines were done together.

Supplementary figure 1

(a) and **(b)** Stomatal response to CO_2 concentration changes from 400 to 800 ppm, 800 to 400 ppm and 400 to 100 ppm, mean stomatal conductance ± SEM is shown. **(c,e)** Boxplot of stomatal conductance (g_s) change (mmol m^{-2} s^{-1}) in response to CO_2 concentration changes from 400 to 800 ppm, 800 to 400 ppm and 400 to 100 ppm, respectively. **(d,f)** Boxplot of fitted k-values (rate constants) of stomatal response to CO_2 concentration changes from 400 to 800 ppm, 800 to 400 ppm and 400 to 100 ppm, respectively, linear responses are marked as NA (not applicable). **(c-f)** Boxes represent 25-75 % quartiles and median as the horizontal lines, whiskers indicate the smallest and largest values, points show individual plant values. Statistically significantly different groups are marked with different letters (One-way ANOVA with Tukey *post hoc* test). **(a-f)** Sample size was 5 for all plant lines. VPD during

experiments was 0.9 kPa in **(a-f)**. Start of first treatment was between 11:30 to 12:30. Col-0 data is same as used in figure 1, experiments with Col-0 and mutant lines were done together.

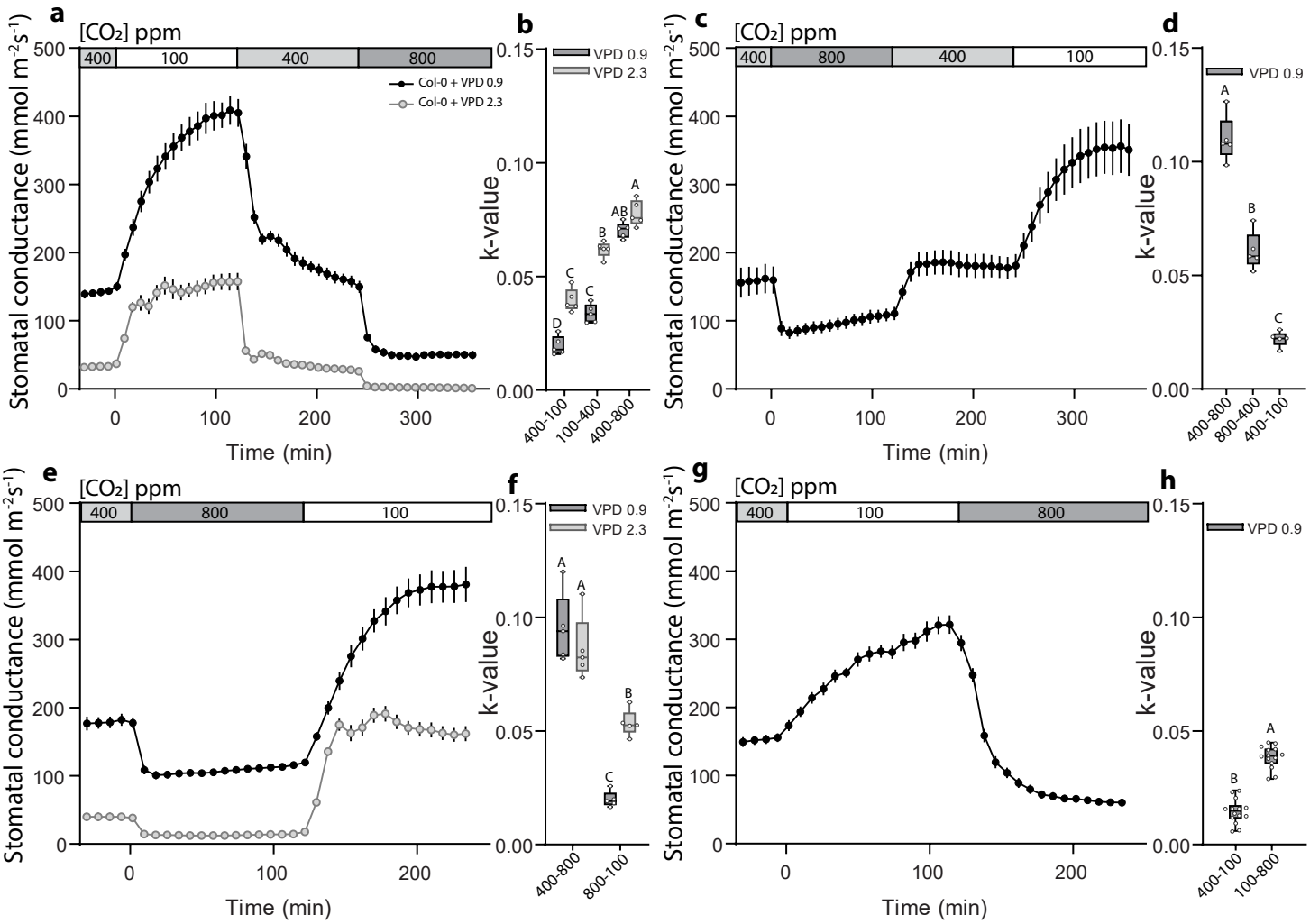

Figure 1. Kinetics of CO_2-induced stomatal closure in wild-type Arabidopsis with regular and elevated VPD.

Col-0 wild-type Arabidopsis stomatal response to sequential changes in CO_2 concentration under regular **(a,c,e,g)** and elevated **(a,e)** VPD conditions. Mean stomatal conductance ± SEM is shown. **(b,d,f,h)** Boxplot of fitted k-values (rate constants) of stomatal response to CO_2 concentration changes. Boxes represent 25-75 % quartiles and median as the horizontal lines, whiskers indicate the smallest and largest values, points show individual plant values. **(b,f)** Statistically significantly different groups are indicated with different letters (Two-way ANOVA with Tukey post-hoc test). **(d,h)** Statistically significantly different groups are indicated with different letters (One-way ANOVA with Tukey *post-hoc* test). Sample size was 5 in **(a,b,c,d,e,f)** and 14 in **(g,h)**. Start of first treatment was between 11:30 to 12:30.

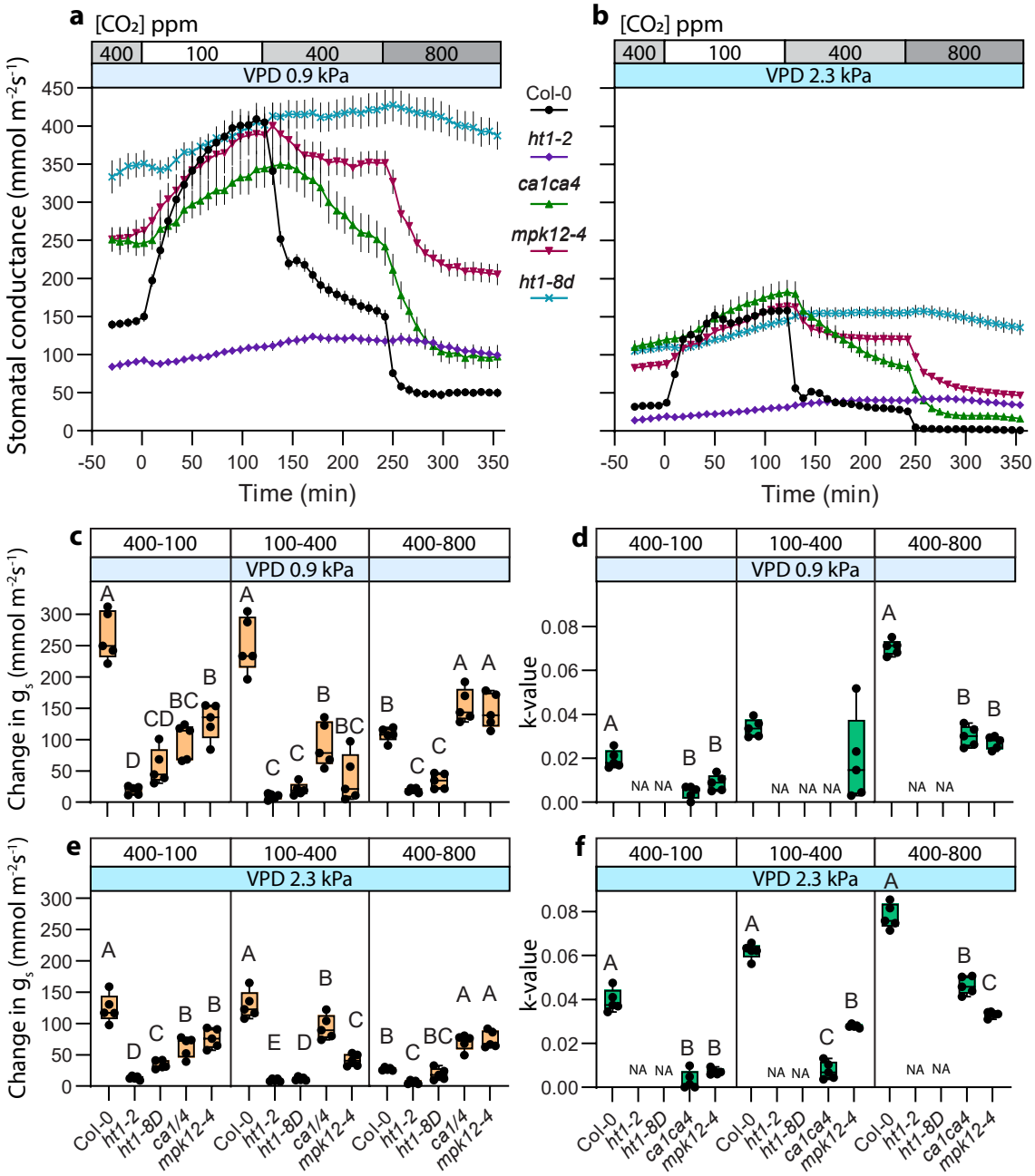

Figure 2. CO_2 pathway mutants retain response patterns under regular and elevated VPD conditions

(a) and **(b)** Stomatal response to CO_2 concentration changes from 400 to 100 ppm, 100 to 400 ppm and 400 to 800 ppm under regular **(a)** and elevated **(b)** VPD conditions, mean stomatal conductance ± SEM is shown. **(c,e)** Boxplot of stomatal conductance (g_s) change (mmol m^{-2} s^{-1}) in response to CO_2 concentration changes from 400 to 100 ppm, 100 to 400 ppm and 400 to 800 ppm, respectively. **(d,f)** Boxplot of fitted k-values (rate constants) of stomatal response to CO2 concentration changes from 400 to 100 ppm, 100 to 400 ppm and 400 to 800 ppm, respectively, linear responses are marked as NA (not applicable). **(c-f)** Boxes represent 25-75 % quartiles and median as the horizontal lines, whiskers indicate the smallest and largest values, points show individual plant values. Statistically significantly different groups are marked with different letters (One-way ANOVA with Tukey *post hoc* test). **(a-f)** Sample size was 5 for all plant lines. VPD during experiments was 0.9 kPa in **(a,c,d)** and 2.3 kPa in **(b,e,f)**. Start of first treatment was between 11:30 to 12:30. Col-0 data is same as used in figure 1, experiments with Col-0 and mutant lines were done together.

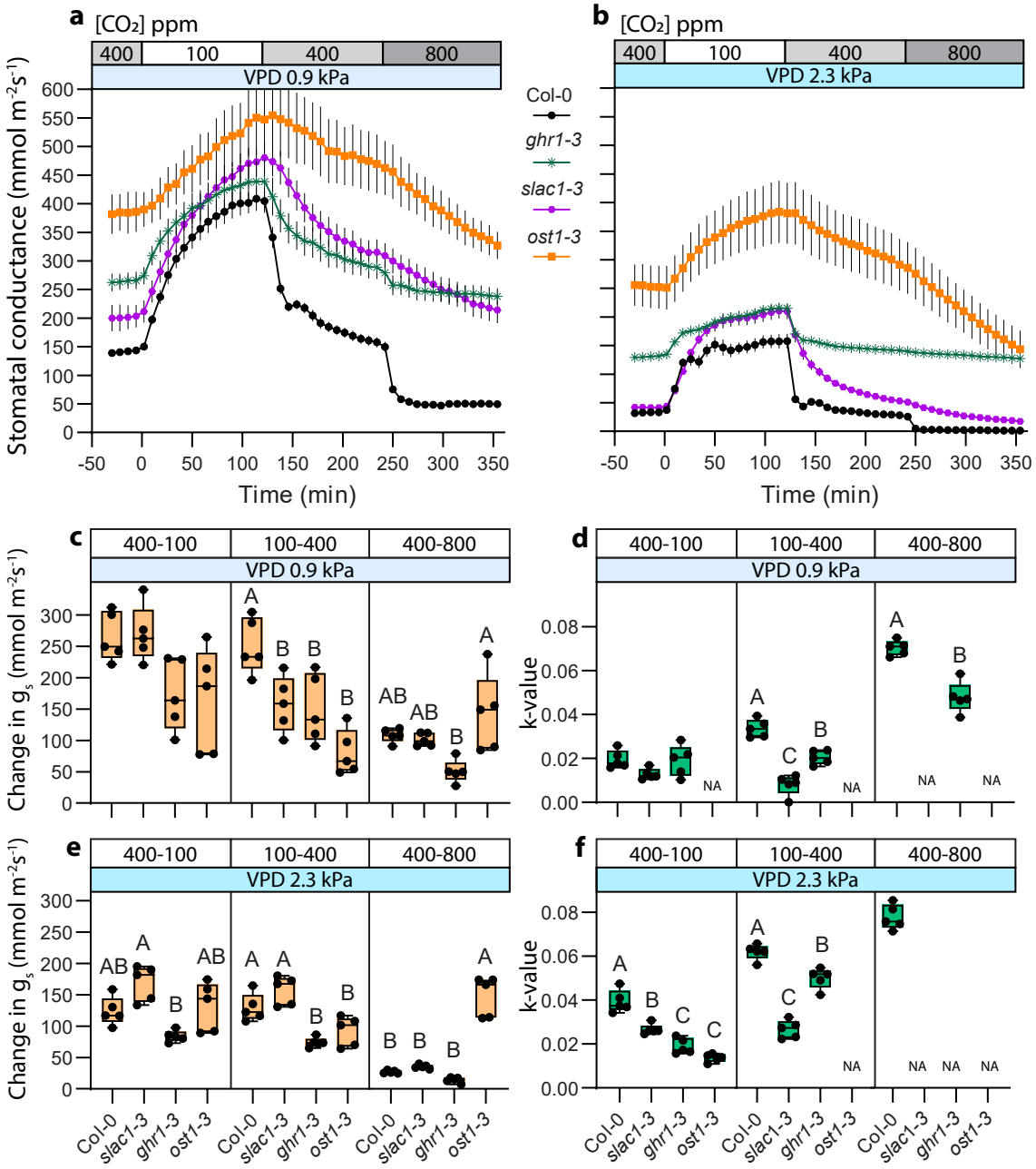

Figure 3. CO_2 response patterns in anion channel activation mutants are affected by VPD conditions

(a) and **(b)** Stomatal response to CO_2 concentration changes from 400 to 100 ppm, 100 to 400 ppm and 400 to 800 ppm in regular **(a)** and elevated **(b)** VPD conditions, mean stomatal conductance ± SEM is shown. **(c,e)** Boxplot of stomatal conductance (g_s) change (mmol m^{-2} s^{-1}) in response to CO_2 concentration changes from 400 to 100 ppm, 100 to 400 ppm and 400 to 800 ppm, respectively. **(d,f)** Boxplot of fitted k-values (rate constants) of stomatal response to CO_2 concentration changes from 400 to 100 ppm, 100 to 400 ppm and 400 to 800 ppm, respectively, linear responses are marked as NA (not applicable). **(c-f)** Boxes represent 25-75 % quartiles and median as the horizontal lines, whiskers indicate the smallest and largest values, points show individual plant values. Statistically significantly different groups are marked with different letters (One-way ANOVA with Tukey *post hoc* test). **(a-f)** Sample size was 5 for all plant lines. VPD during experiments was 0.9 kPa in **(a,c,d)** and 2.3 kPa in **(b,e,f)**. Start of first treatment was between 11:30 to 12:30. Col-0 data is same as used in figure 1, experiments with Col-0 and mutant lines were done together.

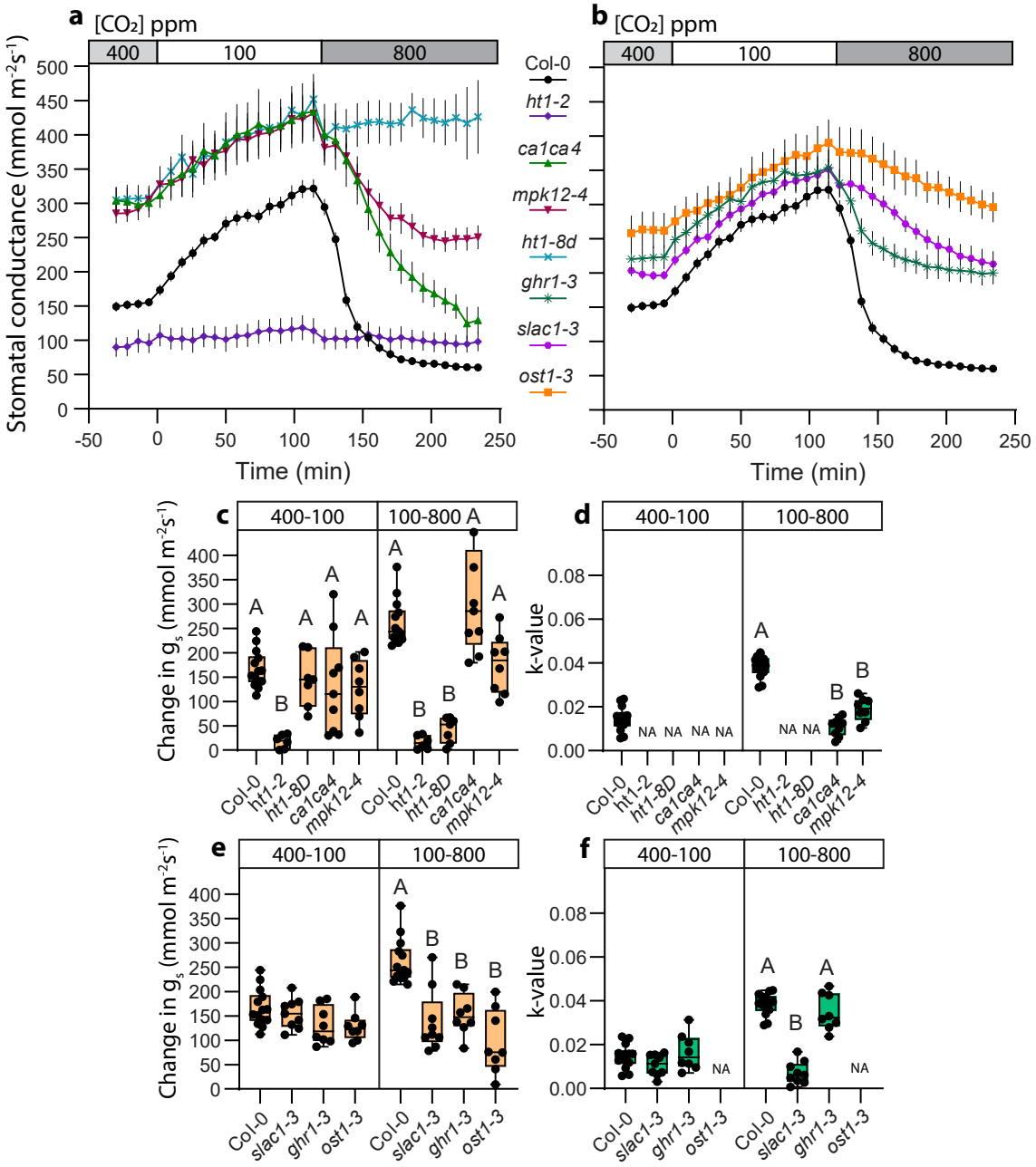

Figure 4. CO_2 transition from 100 to 800 ppm masks different responses present in 100 to 400 and 400 to 800 ppm CO_2 transitions

(a) and **(b)** Stomatal response to CO_2 concentration changes from 400 to 100 ppm and 100 to 800 ppm, mean stomatal conductance ± SEM is shown. **(c,e)** Boxplot of stomatal conductance (g_s) change (mmol m^{-2} s^{-1}) in response to CO_2 concentration changes from 400 to 100 ppm and 100 to 800 ppm, respectively. **(d,f)** Boxplot of fitted k-values (rate constants) of stomatal response to CO_2 concentration changes from 400 to 100 ppm and 100 to 800 ppm, respectively, linear responses are marked as NA (not applicable). **(c-f)** Boxes represent 25-75 % quartiles and median as the horizontal lines, whiskers indicate the smallest and largest values, points show individual plant values. Statistically significantly different groups are marked with different letters (One-way ANOVA with Tukey *post hoc* test). **(a-f)** Sample size was 14 for Col-0; 6 for *ht1-2*; 7 for *ht1-8D*; 8 for *ghr1-3*, *mpk12-4* and *ost1-3*; 9 for *slac1-3* and *ca1ca4*. VPD during experiments was 0.9 kPa in **(a-f)**. Start of first treatment was between 11:30 to 12:30. Col-0 data is same as used in figure 1, experiments with Col-0 and mutant lines were done together.

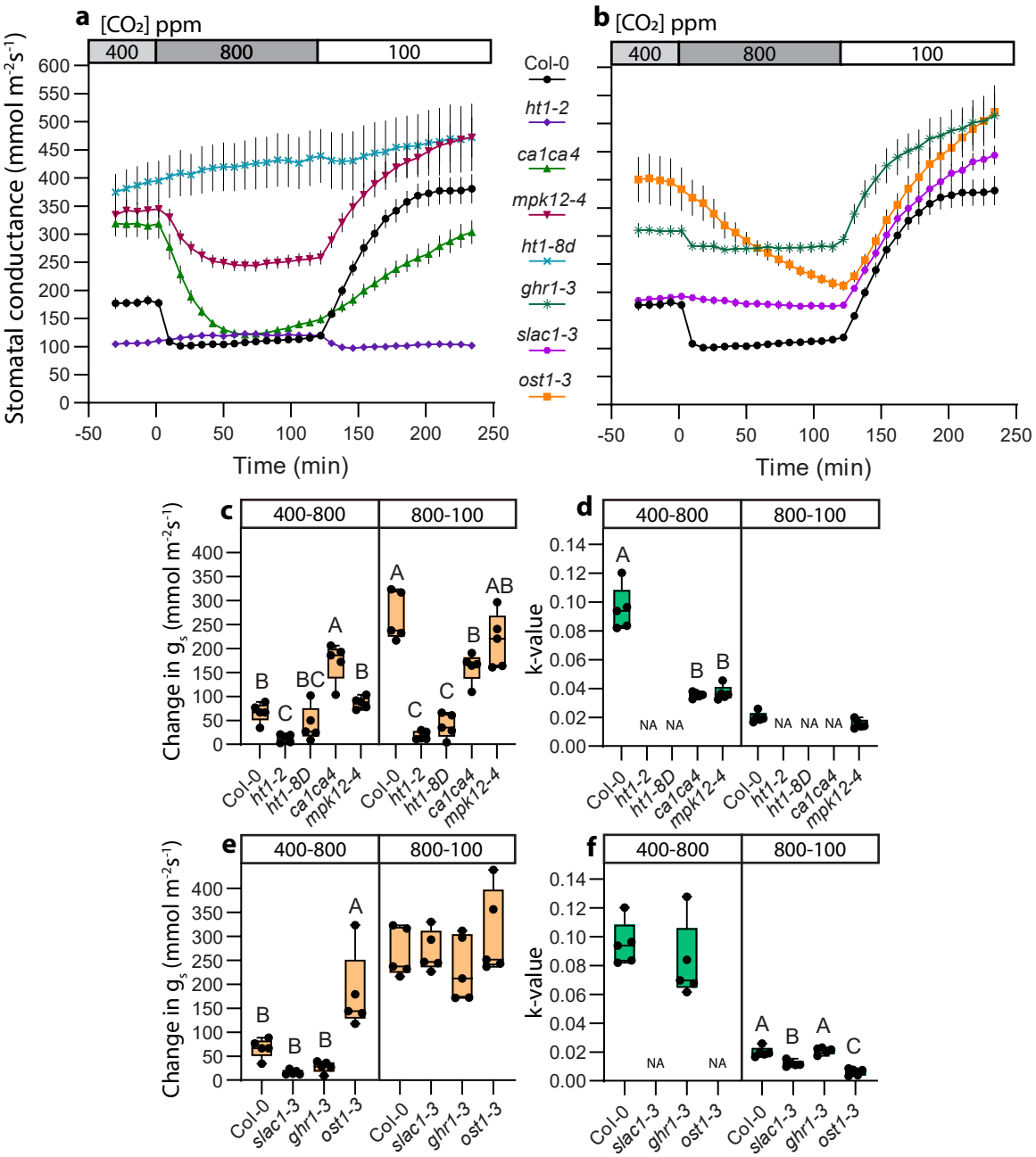

Figure 5. Stomatal opening in 800 to 100 ppm CO_2 transition masks different responses present in sub-ambient and above ambient CO_2 concentrations

(a) and **(b)** Stomatal response to CO_2 concentration changes from 400 to 800 ppm and 800 to 100 ppm, mean stomatal conductance ± SEM is shown. **(c,e)** Boxplot of stomatal conductance (g_s) change (mmol m^{-2} s^{-1}) in response to CO_2 concentration changes from 400 to 800 ppm and 800 to 100 ppm, respectively. **(d,f)** Boxplot of fitted k-values (rate constants) of stomatal response to CO_2 concentration changes from 400 to 800 ppm and 800 to 100 ppm, respectively, linear responses are marked as NA (not applicable). **(c-f)** Boxes represent 25-75 % quartiles and median as the horizontal lines, whiskers indicate the smallest and largest values, points show individual plant values. Statistically significantly different groups are marked with different letters (One-way ANOVA with Tukey *post hoc* test). **(a-f)** Sample size was 5 for all plant lines. VPD during experiments was 0.9 kPa in **(a-f)**. Start of first treatment was between 11:30 to 12:30. Col-0 data is same as used in figure 1, experiments with Col-0 and mutant lines were done together.

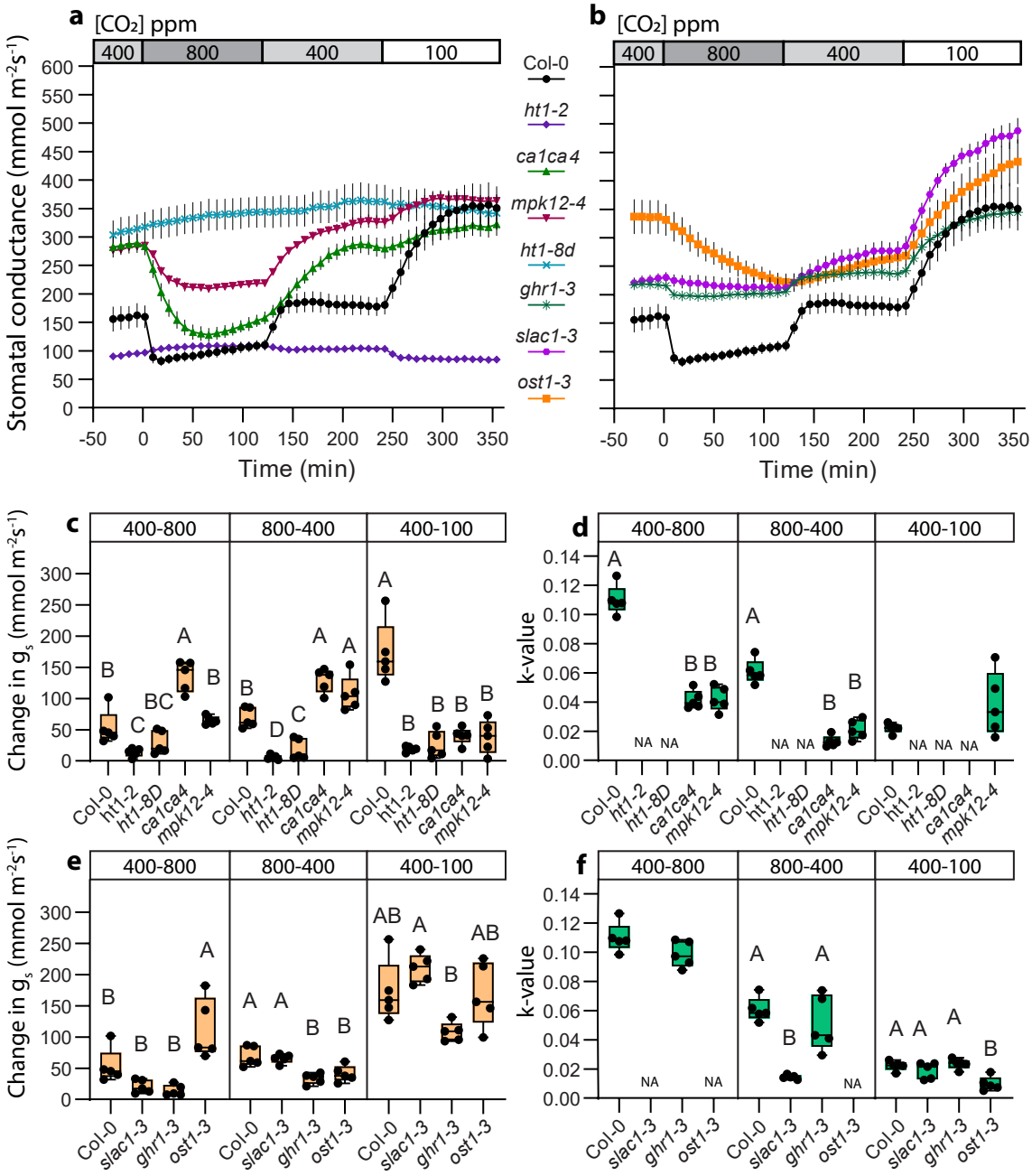

Supplementary figure 1

(a) and **(b)** Stomatal response to CO_2 concentration changes from 400 to 800 ppm, 800 to 400 ppm and 400 to 100 ppm, mean stomatal conductance ± SEM is shown. **(c,e)** Boxplot of stomatal conductance (g_s) change (mmol m^{-2} s^{-1}) in response to CO_2 concentration changes from 400 to 800 ppm, 800 to 400 ppm and 400 to 100 ppm, respectively. **(d,f)** Boxplot of fitted k-values (rate constants) of stomatal response to CO_2 concentration changes from 400 to 800 ppm, 800 to 400 ppm and 400 to 100 ppm, respectively, linear responses are marked as NA (not applicable). **(c-f)** Boxes represent 25-75 % quartiles and median as the horizontal lines, whiskers indicate the smallest and largest values, points show individual plant values. Statistically significantly different groups are marked with different letters (One-way ANOVA with Tukey *post hoc* test). **(a-f)** Sample size was 5 for all plant lines. VPD during experiments was 0.9 kPa in **(a-f)**. Start of first treatment was between 11:30 to 12:30. Col-0 data is same as used in figure 1, experiments with Col-0 and mutant lines were done together.